

## Blast Diffusion by Different Shapes of Domes

Ram Ranjan Sahu\* and Pramod Kumar Gupta

*\*Tata Motors, Pune, India*

*Indian Institute of Technology Roorkee-247 667, India*

*\*E-mail: RamRanjan.Sahu@tatatechnologies.com*

### ABSTRACT

Domes have been used since ancient times in constructions. These are effective structures in supporting loads for large span. Dome has an added advantage of having good looking in structural applications. Many shapes of domes are being used nowadays for residential, commercial, and industrial purposes. Specific purpose domes are also used for nuclear containment. Main threats to structures are from the bomb blast. Hence, domes too are to be designed to withstand effectively the pressure energy generated by the blast. A comparative theoretical study is proposed on the different shapes of domes having same weight and thickness. Various responses are estimated through numerical method after simulating blast and comparing their intensities.

**Keywords:** Domes, energy of explosion, TNT equivalent mass, energy dissipation, finite element analysis

### 1. INTRODUCTION

In recent past the terrorist attacks have been more frequent on residential and commercial setups. Hence, the research on protection against blast threats to buildings and personnel have been an increasing role. Many researchers have been studying the complicated chemistry of the blast and designing effective structural shapes to mitigate the blast energy.

Zhai<sup>1</sup>, *et al.* studied the single-layer reticulated dome spanning over 40 m subjected to eccentric blast loading. The authors used Finite Element simulation to reproduce the process of detonation of the explosive charge to the demolition of reticulated dome structures. Authors discussed about the approaches to improve the blast-resistant capacity of reticulated dome and response under eccentric blast loadings. Authors also discovered that the partially reinforcement of reticulated dome is an effective and economical way to improve its blast-resistant capacity compared with fully reinforced reticulated dome. The provision of openings on the wall to mitigate the blast loading was also discussed. Ngo<sup>2</sup>, *et al.* presented a comprehensive overview of the effects of explosion on structures. An explanation of the nature of explosions and the mechanism of blast waves in free air is given. Author's paper also introduced different methods to estimate blast loads and structural response. Olson<sup>3</sup>, *et al.* and Nurick<sup>4</sup> analysed stiffened and un-stiffened clamped square mild steel plates under uniformly distributed blast load. The strain rate sensitivity was predicted to un-stiffened plates in different modes. Different approaches to the numerical analysis of the blast event are presented and results are compared. In particular the blast load is applied using the standard engineering model (CONWEP) because of the obvious computational advantages of this approach. Many

guidelines are laid in manuals for fundamentals of protective design for conventional weapons. One such manual is TM 5-855-1<sup>5</sup> by U.S. Department of Army. This manual provides the procedures for the design and analysis of protective structures subjected to the effects of conventional weapons. Neuberger<sup>6</sup> *et al.* studied the response of circular plates subjected to spherical explosions. Author's study presented numerical and experimental results from a series of controlled explosion experiments. The first part of author's paper deals with spherical charges exploding in free air, while the second part deals with the same charges flush-buried in dry sand. A good agreement between numerical simulation predictions and test results was obtained. The Authors used scaled models for the study by replicating all geometrical parameters, while the blast effect was scaled using the Hopkinson Scaling Law, which relates the physical dimensions between different explosives charges of the same material. The overall effect of the strain rate sensitivity and variability of material properties with plate thickness were considered on the response of the scaled model. Wen and Jones<sup>7</sup> found the geometrical scalability on metal plates subjected to impact. The authors also investigated in their experiment, that the scaling is insensitive to strain rate. Scaling aspects were also studied by Jacob<sup>8</sup>, *et al.* on quadrangular plates subjected to localised blast loads. The authors investigated the effects of varying the charge weight and plate geometries on the deformation. Authors introduced a dimensionless number to represent the quadrangular plate's response to a localised disc charge.

In this paper different shapes of domes with same weight (0.9 kg) and thickness (2 mm) are taken for analytical study. The same weight and thickness are the basic assumptions with

which different shapes of domes are made and blast response are compared. Their finite element (FE) models with dimensions are shown in Fig. 1. These were subjected to blast of same charge (TNT equivalent mass) at their mid-height, at inside. The mid-height is considered so that the blast effect reaches every inner portion of dome. Here, assumptions are made that the dome coordinate system lies to the centre of base circle and Z is vertical coordinate system. The FE models were used to calculate the weight of the domes by summing up the weight of all solid elements used for building a dome.

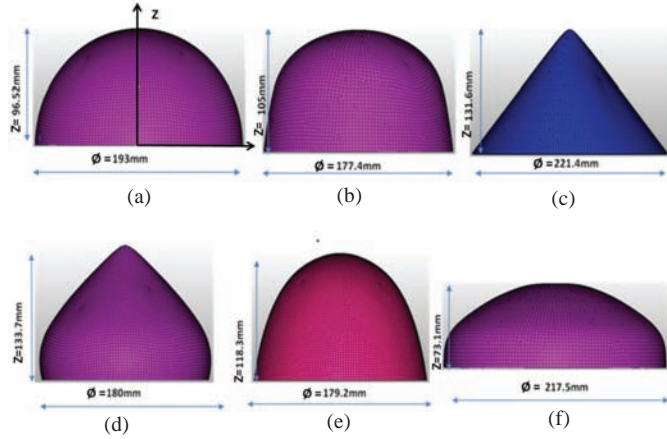


**Figure 1. Different FE models of domes; (a) Circular, (b) Bowl, (c) Triangular, (d) Pointed, (e) Parabolic, and (f) Shallow.**

## 2. FINITE ELEMENT SIMULATION

### 2.1 FE Setup

The Finite Element (FE) models of the domes were generated by HyperMesh<sup>9</sup>. The domes volumes were FE modelled with solid elements with size of 2.25 mm. The element counts are from 40000 to 55000 elements, depending upon dome geometry. Since the domes have simple curvature, this element size (2.25 mm) is fine enough to capture the minute geometrical details of the domes and cladding well to the geometries of domes, as shown in Fig. 1. Also this element size ensures good convergence and less deviation to output parameters. The elements chose were reduced integration solid elements (LS-DYNA element formulation 2). The solid elements were of hexagonal and pentagonal shapes. The 3 rows of elements were ensure in the thickness direction to take care the out-of-plane shear and smooth transition of responses across thickness The 3-D FE models of the domes were analysed using the nonlinear explicit code LS-Dyna<sup>10</sup>, which takes into account both material nonlinearity and geometric nonlinearity.

CONWEP load function was applied to generate the blast equivalent pressure distribution on the dome. In LS-DYNA CONWEP<sup>11</sup> function is called with \*LOAD\_BLAZT card. This card uses computer program CONWEP which assumes the following exponential decay of the pressure with time.

$$p(t) = p_{s0} \left[ 1 - \frac{t - T_{\alpha}}{T_0} \right] e^{-\frac{A(t - T_{\alpha})}{T_0}} \quad (1)$$

where  $p(t)$  [kPa] is the pressure at time  $t$ ,  $p_{s0}$  [kPa] is the peak

incident pressure,  $T_0$  [ms] is the positive phase duration,  $A$  is the decay coefficient (dimensionless) and  $T_{\alpha}$  [ms] is the arrival time. The TNT equivalent mass (0.15 kg), stand-off distance (charge at centre mid-height of dome) and type of burst (air burst) are the input requirement and supplied appropriately while solving. The LS-Dyna \*LOAD\_BLAZT card used is based on a report by Randers-Pehrson and Bannister<sup>12</sup>. This option determines the pressure values when used in conjunction with the keywords \*LOAD\_SHELL.\*Load\_Body was used to take accountability of gravitational load and \*Load\_Segment was used to apply pressure on inner surface of dome.

### 2.2 Material Modeling

The material model Johnson\_Cook was used to define the dome steel material. This is material type 15 in LS-Dyna. This material is applicable to the high rate deformation of many materials including most metals. The typical application includes explosive metal forming, ballistic penetration, and impact.

This material is used to take accountability of strain and temperature-sensitive plasticity. The strain rates variation over a large range and adiabatic temperature increases due to plastic heating leads material softening. This material is implemented in LS-Dyna with \*MAT\_015 card. Johnson\_Cook constitutive equation can be represented by the following equation:

$$p = \rho_0 C^2 \mu + (\gamma_0 + \alpha \mu) E \quad (2)$$

where  $\epsilon$  is the effective plastic strain,  $\dot{\epsilon}$  is the total strain rate,  $\epsilon_0$  is the reference plastic strain rate,  $T$  is the temperature of the work material,  $T_m$  is the melting temperature of the work material and  $T_{room}$  is the room temperature. Coefficient  $A$  is the strain hardening constant,  $B$  is the strain hardening coefficient,  $C$  is the strain rate coefficient,  $n$  is the strain hardening exponent and  $m$  is the thermal softening exponent.

The strain at fracture is given by:

$$\epsilon^f = \left[ D_1 + D_2 e^{D_3 \sigma^*} \right] \left[ 1 + D_4 \ln \epsilon^* \right] \left[ 1 + D_5 \left[ \frac{T - T_{room}}{T_{melt} - T_{room}} \right] \right] \quad (3)$$

where  $D_i, i=1 \dots 5$  are input constants,  $\sigma^*$  is the ratio of pressure divided by effective stress ( $\sigma^* = p/\sigma$ ) and  $\epsilon^*$  is the ratio of effective total strain rate normalised by reference plastic strain rate. Fracture occurs when the damage parameter  $D = \sum (\Delta \epsilon) / \epsilon^f$  reaches the value of 1. This is similar in form to the yield strength model with three terms combined in a multiplicative manner to include the effect of stress triaxiality, strain rate and local heating, respectively.

When this material is used with solid elements, this model requires an equation-of-state (EOS) to define a relation between the pressure and the volume of a solid at a given temperature. Gruneisen developed a law which explains the physics that governs the behaviour of solids under above-mentioned circumstances. The ratio of the coefficient of expansion of a metal to its specific heat at constant pressure is constant at all temperatures. It has developed over the years with a concern to get an analytical expression to the law. A thermodynamic state of a homogeneous material which is not undergoing any chemical reactions or phase changes may be defined by two state variables is called an equation of state. The Gruneisen

equation of state with cubic shock velocity-particle velocity ( $v_s - v_p$ ) defines pressure for compressed material as

$$p = \frac{\rho_0 c^2 \mu \left[ 1 + \left( 1 - \frac{\gamma_0}{2} \right) \mu - \frac{\alpha}{2} \mu^2 \right]}{\left[ 1 - (s_1 - 1) \mu - s_2 \frac{\mu^2}{\mu + 1} - s_3 \frac{\mu^3}{(\mu + 1)^2} \right]^2} + (\gamma_0 + \alpha \mu) E \quad (4)$$

where  $C$  is the intercept of the  $v_s - v_p$  curve;  $S_1$ ,  $S_2$  and  $S_3$  are the coefficients of the slope of  $v_s - v_p$  curve;  $\gamma_0$  is the Gruneisen gamma;  $\alpha$  is the first-order volume correction to  $\gamma_0$ ,  $E$  is the internal energy per unit volume and  $\mu = \rho / (\rho_0 - 1)$ .

The compression is defined in terms of the relative volume,  $V$  as:

$$\mu = \frac{1}{V} - 1$$

For expanded materials as the pressure is defined by:

$$p = \rho_0 C^2 \mu + (\gamma_0 + \alpha \mu) E \quad (5)$$

The values for Johnson-Cook material (Mat 015) model and Gruneisen EOS (equation of state) parameters taken in this problem are shown in Table 1.

**Table 1. Johnson-Cook material model and Gruneisen EOS**

Johnson-Cook material (Mat 015)			
Density [kgmm <sup>-3</sup> ]	7.8e-6	$T_m$ [K]	1800
Young's Modulus, E [GPa]	210	$T_{room}$ [K]	280
Shear Modulus, G [GPa]	80	Reference Plastic Strain Rate [s <sup>-1</sup> ]	1e <sup>-5</sup>
Poisson's Ratio	0.3	Specific Heat [J/kgK]	450
Strain Hardening Constant, A [GPa]	0.849	Failure parameter D1	0.020
Strain Hardening Coefficient, B [GPa]	1.340	Failure parameter D2	1.5
Strain Rate Coefficient, C	0.03	Failure parameter D3	0.2
Strain Hardening Exponent, $n$	0.092	Failure parameter D4	0.002
Thermal Softening Exponent, $m$	0.870	Failure parameter D5	0.0
*EOS_GRUNEISEN			
C [m/s]	4569	S3	0
S1	1.49	$\gamma_0$	2.17
S2	0	A	0

### 2.3 Load and Boundary Conditions

The domes are rigidly fixed at the base. The TNT equivalent of 0.15 kg is blasted inside at the centre, at mid height of dome and various responses are estimated for 2 ms. The charge of 0.15 kg could work out to initiate the structural rupture in most of the domes. The time period of 2 ms was sufficient to stabilise the response and capture the blast phenomenon.

## 3. RESULTS

The aftereffect of blast in terms of energy balance, dome's distortion and inside pressure response at different locations are discussed in details.

### 3.1 Energy Balance

The FE result correctness is judged by energy balance of the system. The unwanted energy like hourglass and sliding energies were kept less which is pre requisite of the simulation. The total energy contribution is ensured only through kinetic energy (KE) and internal energy (IE) of the material.

### 3.2 Deformation Response

The blast deformation response of various domes at 0.2ms is shown in Fig. 2. The enlargement is not scaled here and shown with original dimensions. It is clear from the figure that the bowl and parabolic shape domes could sustain the blast, while other domes could not. Other domes are tearing at the top. The triangular dome is tearing up to its bottom, which can be said that it has undergone maximum damage.

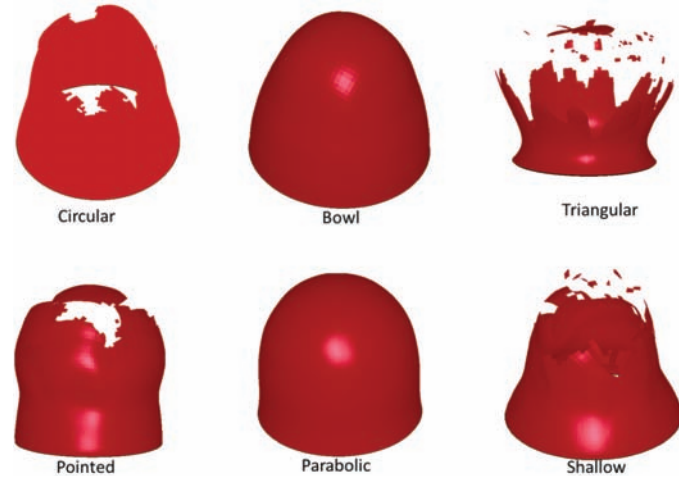


**Figure 2. Deformation response of the domes at 0.2 ms.**

### 3.3 Pressure Response

The pressure variation were observed at top, mid and bottom positions on dome's inside. Figure 3(a) shows these 3 locations and wave propagation after blast. The pressure variation is shown in Fig. 3(b) for circular, bowl, and triangular shape domes. The domes are shown in left side while pressure variation at right side. The inside elements (mark by 'H' followed by element number) for pressure measurement at three locations are also shown on domes. It is observed that the maximum pressure for circular dome is at mid location, followed by top and bottom positions. Mid-position pressure variation is less for bowl shape dome compared to circular shape dome. The bottom position pressure variation is more for triangular dome.

## 4. DISCUSSIONS

The domes with same weight and thickness were subjected to blast pressure inside. The shape, quantity of TNT and its position inside the dome play important roles in the blast interaction. These are discussed as below.

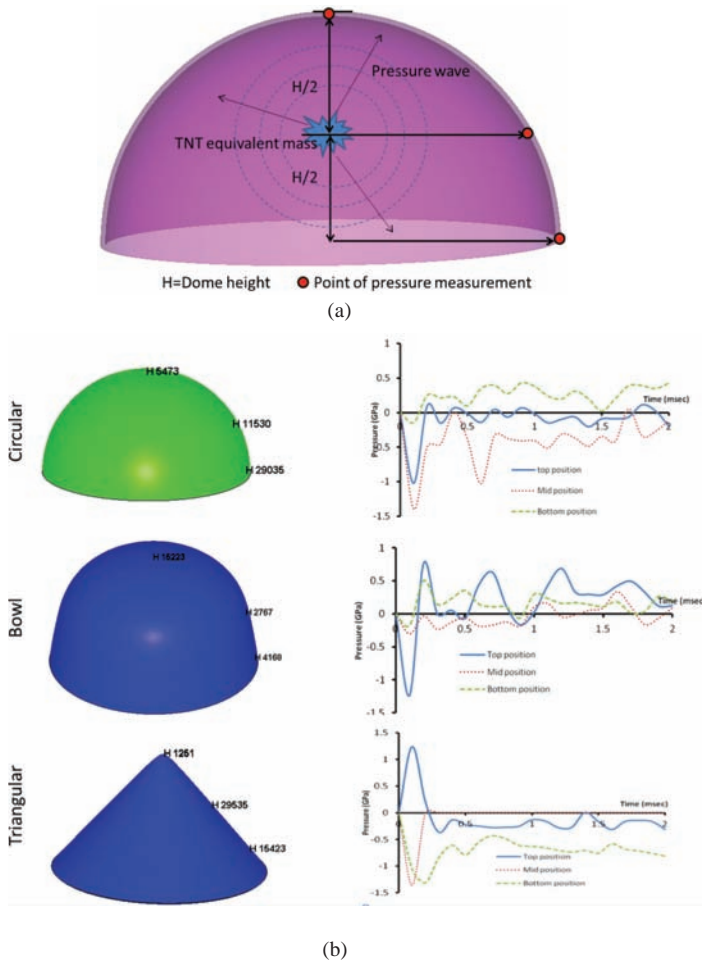


Figure 3. Pressure measurement; (a) Points of measurement, (b) Pressure response at different locations.

#### 4.1 Top of Domb Displacement

The resultant displacement of top of the dome are estimated and shown in Fig. 4. Since the parabolic and bowl shaped dome did not burst, their top position displacement is minimum (58mm) among all domes. The maximum displacement (1219mm) is observed for triangular dome.

#### 4.2 Dome Mid Acceleration with Various TNT Quantities

The acceleration is estimated at mid location (node number 32554) of circular dome for various amounts of TNT (0.3 kg, 0.2 kg, 0.15 kg, and 0.1 kg) as shown in Fig. 5. It is obvious from the figure that more amount of TNT generates more acceleration, as expected.

#### 4.3 Internal and Kinetic Energy of Domes

The material internal and kinetic energy of various domes were estimated and compared as shown in Fig. 6. The parabolic dome has maximum internal energy because it did not burst, rather it sustains the burst pressure by undergoing enlargement at top portion (Fig. 2) causing more strain in the elements and thereby generates more internal energy. Owing to the shape of triangular dome, the sides are near-to-blast charge, and hence, it experiences more kinetics and strains, causing higher internal and kinetic energy. The bowl and parabolic shape domes did

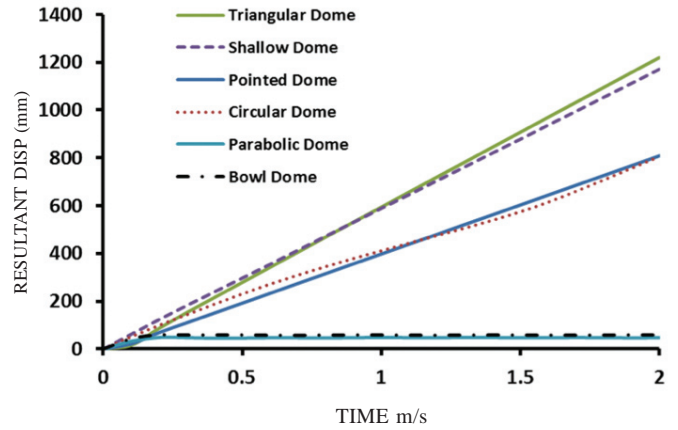
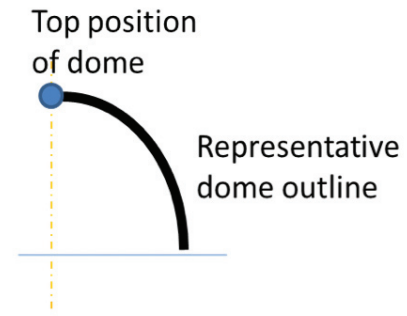


Figure 4. Resultant displacement of the top position of domes.

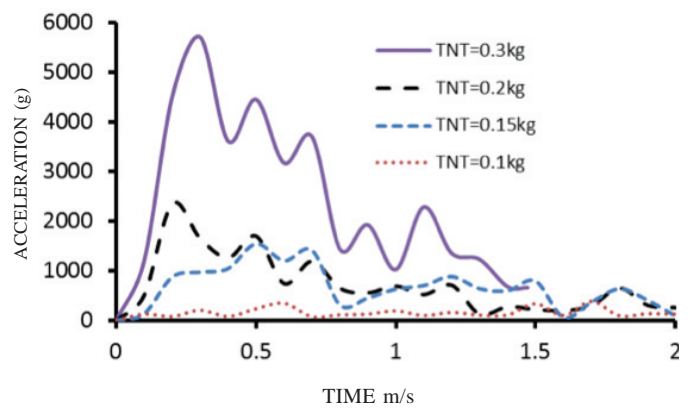
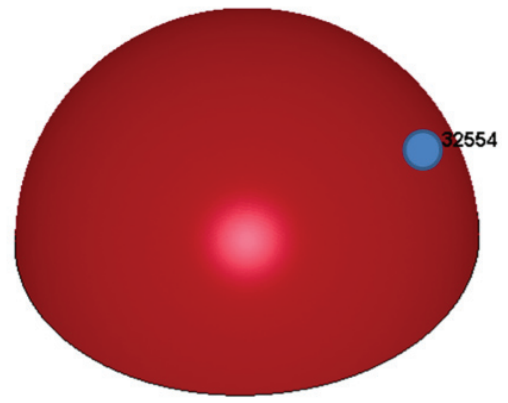
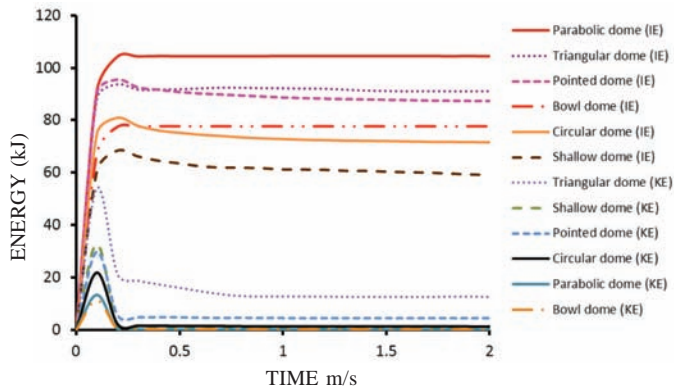


Figure 5. Mid position acceleration of circular dome.



**Figure 6. Internal and Kinetic energy comparison for various domes.**

not burst and hence shows least kinetic energy as compared to others. Shallow dome top is nearer to blast charge as compared to other domes and hence more kinetic energy is also observed for it.

#### 4.4 Response with Various Positions of Blast Charge

The position of blast charge plays an important role in aftereffect of blast. The circular dome is blasted in three locations, i.e. at base, mid-height, and near top position (10 mm below inner surface). The blast responses in terms of internal energy (IE) and kinetic energy (KE), at these three positions are shown in Fig. 7. The deformation responses at 0.2 ms are shown along with graphs. The dome did not damage when it is blasted at base, while it gets damage in other two cases. The blast at top position leads more kinetic energy as compared to base and mid-position blasts. The least internal energy and kinetic energy is observed for the blast at the base. The blast at the mid causes stretching at mid portion elongating the dome and then it burst at the top. This causes more internal energy as compared to others.

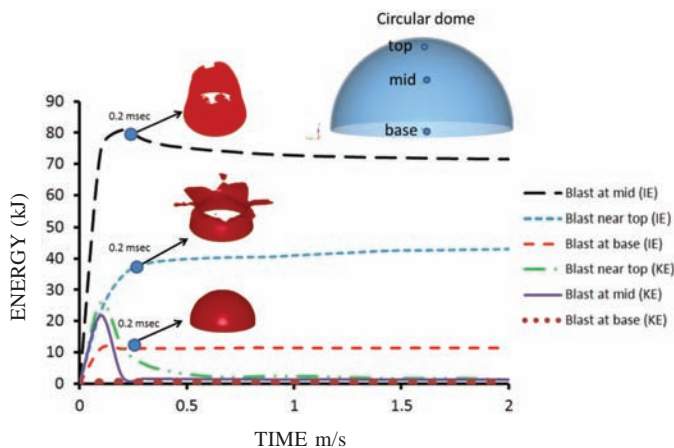


**Figure 7. Blast response of circular dome to various position of blast charge.**

## 5. CONCLUSIONS

Comparative theoretical study on blast (inside) response is performed on the different shapes of domes of same weight and thickness. The hypermesh could be used for FE model building while LS-Dyna used as solver. The LS-Dyna capability to

simulate blast load and material non linear modelling could be effectively used in analysis. The study shows that the parabolic and bowl shape domes could withstand the blast load with least top displacement. These domes have maximum internal energy and least kinetic energy on blast. Study also shows that the mid-location blast causes more damage to the domes. For the future scope, a comparative study can be made on different types of domes by keeping the critical parameters the same like explosive charge weight, type of charge and standoff distance. Also the analysis could be expanded for the reinforced cement concrete domes.

The loading caused by blast pressure and structural distortion response of a particular dome is attributed to its geometry. The curvature of the dome gives rise to convergence or divergence of the pressure waves that are incident on it. This pressure propagation nature with different shapes of domes could be taken for future scope of study.

## ACKNOWLEDGEMENTS

The authors gratefully acknowledges the support of Engineering Research Centre of Tata, Pune for the support for analytical works. Also thanks to the CAD Group to provide the necessary support to build the domes geometry.

## REFERENCES

- Zhai, X.; Wang, Y. & Huang, M. Performance and protection approach of single-layer reticulated dome subjected to blast loading. *Thin-Walled Structure*, 2013, **73**, 57-67. doi: 10.1016/j.tws.2013.07.011
- Ngo, T.; Mendis, P.; Gupta, A. & Ramsay, J. Blast loading and blast effects on structures: An overview. *Electr. J. Struct. Engg.*, Loading on Structures. The University of Melbourne, Australia, 2007.
- Olson, M. D.; Nurick, G. N & Fagnan, J. R. Deformation and rupture of blast-loaded square plates-predictions and experiments. *Int. J. Impact Engg.*, 1993, **13**(2), 279-91. doi: 10.1016/0734-743X(93)90097-Q
- Nurick, G. N. Deformation and tearing of blast-loaded stiffened square plates. *Int. J. Impact Engg.*, 1995, **16**(2) 273-91. doi: 10.1016/0734-743X(94)00046-Y
- 'Fundamentals of Protective Design for Conventional Weapons', U.S. Department of the Army, Washington DC, 1986. TM 5-855-1
- Neuberger, A.; Peles, S. & Rittel, D. Scaling the response of circular plates subjected to large and close-range spherical explosions. Part I: Air-blast loading. *Int. J. Impact Engg.*, 2007, **34**(5), 859-73. doi: 10.1016/j.ijimpeng.2006.04.001
- Wen, H. M. & Jones, N. Experimental investigation of the scaling laws for metal plates struck by large masses. *Int. J. Impact Engg.*, 1993, **13**(3), 485-05. doi: 10.1016/0734-743X(93)90120-V
- Jacob, N.; Chung, K. Y. S.; Nurick, G. N.; Bonorchis, D.; Desai, S. A. & Tait, D. Scaling aspects of quadrangular plates subjected to localised blast loads experiments and predictions. *Int. J. Impact Engg.*, 2004, **30**(8-9), 1179-208. doi: 10.1016/j.ijimpeng.2004.03.012

9. HyperMesh11 software. A product of Altair Engineering HyperWorks, for finite element pre-processing. www.altairhyperworks.com, 1820 E Big beavers, Troy, MI 48083.
10. LS-DYNA Version 971 R6.1.0. A program for nonlinear dynamic analysis of structures in three dimensions, Livermore Software Technology Corporation, 2012.
11. Hyde, D. W. CONWEP: Conventional Weapons Effects Program. 1991: US Army Engineer Waterways Experiment Station, USA.
12. Randers-Pehrson G. & Bannister, K. A. Airblast loading model for DYNA2D and DYNA3D. Army Research Laboratory (1997), ARL Report No. ARL-TR-1310.

## CONTRIBUTORS



**Dr Ram Ranjan Sahu** received his MTech (Stress and Vibration) from Barkatullah University, Bhopal (MP) and PhD (Structures) from IIT, Roorkee. He is working as Assistant General Manager in Engineering Research Centre (ERC) of TATA Motors, Pune, His fields of interest are design and analysis of Automotive and Aerospace structures.



**Dr Pramod Kumar Gupta** is Professor in Civil Engineering Department of IIT-Roorkee. He has rich teaching experience in structures and has guided many PhD and M. Tech students. He is pioneering concrete field tube technology in India and guiding many students in this subject.